

Table 1. Source of Na, K, Mg, and Ca in various types of rivers.

River	Contribution from precipitation (%)	Contribution from rocks (%)
<i>Rain-dominated river type</i>		
Rio Tefé	81	19
<i>Rock-dominated river type</i>		
Ucayali	4.8	95.2
<i>Evaporation-crystallization river type</i>		
Rio Grande	0.1	99.9

group are usually located in hot, arid regions. A number of these rivers (the Pecos and the Rio Grande are good examples) show evolutionary paths, designated by arrows in Figs. 1 and 3, starting near the Ca or "rock source" end-member with changes in composition toward the Na-rich, high-salinity end-member as the rivers flow toward the ocean. This change in composition and concentration along the length of these rivers is due to evaporation, which increases salinity, and to precipitation of CaCO_3 from solution, which increases the relative proportion of Na to Ca both from the tributaries and in the mainstream.

The Na-rich, high-salinity, end-member components are the various seawaters of the earth whose compositions (Fig. 1) cluster near the Na-rich axis. Seawater, however, cannot evolve simply from the concentration of freshwater and the precipitation of CaCO_3 . Rather, as suggested by several researchers (1, 3, 4), there are other minor mechanisms—in addition to the major mechanisms—evaporation and crystallization—that contribute to the final exact composition of seawater.

Mass balance calculations of the contributions of Na, K, Mg, and Ca into three rivers exemplifying the three types of rivers described are given in Table 1. For each of the three river basins, the amount of dissolved salts contributed by precipitation was calculated from the sum of the concentrations of Ca, Na, K, and Mg multiplied by the annual precipitation. The calculations for precipitation contributions are based on data from chemical analysis of rain (5, 7) and yearly precipitation data (5, 8). The contributions from the rocks of the basins are logically assumed as the difference between river outflow and precipitation contribution. These calculations illustrate the precipitation dominance in the supply by precipitation of 81 percent of the Na, K,

Mg, and Ca carried by the Rio Tefé, an example of the rain-dominated type of river. The Rio Tefé is an Amazon tributary located 1700 km inland from the Atlantic.

The idea that these three major mechanisms—atmospheric precipitation, rock dominance, and the evaporation-crystallization process—control world water chemistry is borne out by a consideration of the major anions of the world's waters: chloride and bicarbonate. A presentation similar to that for the major cations (Fig. 1) is given in Fig. 4 for the major anions and total salinity. This presentation shows trends remarkably similar to those for cations and indicates support for the controlling mechanisms presented. For rivers in arid regions the evolutionary paths from the HCO_3^- end-member to the Cl end-member are again demonstrated by the data for the anions of the Rio Pecos and Rio Grande, plotted as arrows in Fig. 4.

For the axes showing data for total dissolved salts (Figs. 1, 3, and 4), precipitation or runoff data could be substituted without materially altering the interpretation. The great majority of Na-rich rivers and lakes of the world—both the humid and arid groupings of

Figs. 1 and 3—are in warm to hot climates.

In conclusion, these three mechanisms—atmospheric precipitation, rock dominance, and the evaporation-crystallization process—are the major factors controlling the composition of the dissolved salts of the world's waters. Other second-order factors, such as relief, vegetation, and composition of material in the basin dictate only minor deviations within the zones dominated by the three prime factors.

RONALD J. GIBBS

Department of Geological Sciences,
Northwestern University,
Evanston, Illinois 60201

References and Notes

1. E. J. Conway, *Proc. Roy. Irish Acad. Sect. B* **48**, 119 (1942).
 2. E. Gorham, *Geol. Soc. Amer. Bull.* **72**, 795 (1961).
 3. F. T. Mackenzie and R. Garrels, *Science* **150**, 57 (1965); *Amer. J. Sci.* **264**, 507 (1966).
 4. L. G. Sillén, *Science* **156**, 1189 (1967).
 5. R. J. Gibbs, in preparation.
 6. D. A. Livingstone, *U.S. Geol. Surv. Prof. Pap.* **440-G** (1963), pp. 1-63.
 7. J. H. Feth, *U.S. Geol. Surv. Prof. Pap.* **575-C** (1967), p. 223.
 8. H. Bayer, Ed., *World Geographic Atlas* (Container Corporation of America, Chicago, 1953), p. 70.
 9. E. D. Goldberg, in *Chemical Oceanography*, J. P. Riley and G. Skirrow, Eds. (Academic Press, London, 1965), p. 712.
 10. Supported by the Office of Naval Research.
- 14 August 1970

Radar Interferometric Observations of Venus at 70-Centimeter Wavelength

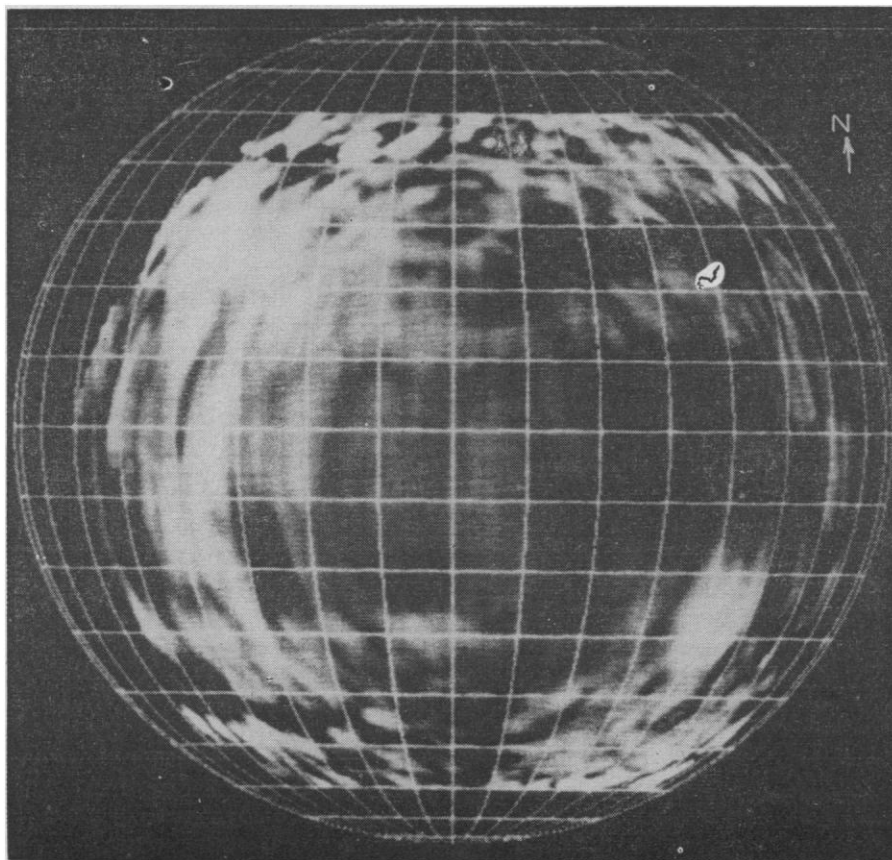
Abstract. *A radar interferometer was used to map unambiguously the surface reflectivity of Venus in the polarized mode at a wavelength of 70 centimeters. The observed region extended from 260° to 30° in longitude and from -60° to 50° in latitude with a surface resolution of approximately 3° by 3°. The result agrees well in most respects with earlier maps made elsewhere at shorter wavelengths and, in addition, discloses a number of new "features."*

When delay-Doppler alone is used for discrimination, the mapping of scattering characteristics of planetary surfaces by Earth-based radar yields an ambiguity in the sign of one coordinate. An interferometer was first used by Rogers *et al.* (1) at Haystack Observatory in 1967 to resolve this ambiguity in Venus echoes at a wavelength of 3.8 cm. At the time of the 1969 inferior conjunction of Venus, greater sensitivity in their radar system enabled Rogers and Ingalls (2, 3) to improve the earlier map of surface scattering.

In this report we describe interferometer observations of Venus made at the Arecibo Observatory in 1969 at a substantially longer wavelength (70 cm)

than was used at Haystack and with coverage of a somewhat larger area of the surface. It was hoped that a comparison between maps at such different wavelengths might yield an indication of the scale sizes of the planetary surface irregularities that are primarily responsible for the backscattered power at large angles of incidence. The Arecibo interferometer that was used to receive the echoes consisted of the basic 1000-foot (300-m) reflector (which was also used as the transmitting antenna) and a fixed parabolic reflector of 100-foot (30-m) diameter, with a movable offset feed that allowed tracking up to 10° from the zenith. The parabola was located 10.8 km to the north-

Fig. 1. Intensity display of the local variations in radar scattering from Venus at 70 cm. The limits of coverage are determined by the signal-to-noise ratio.



northeast of the 1000-foot reflector.

The extent of the planetary surface that was mapped, as well as the resolution, was limited primarily by the sensitivity of the radar system. For this reason the maps do not extend beyond 55° of surface arc from the sub-Earth point on a given day. An effective pulse length of 1.0 msec was transmitted, and a frequency resolution of 0.025 times the maximum planetary (limb-to-limb) Doppler spread was used in the analysis. The resulting linear surface resolution depends on location but is typically 300 km or 3° of surface arc. The transmitted signal was left-circularly polarized but the sense of polarization received was right circular, thus assuring maximum sensitivity of the system to quasi-specularly reflected energy.

Observations of Venus were made on 11 days between 20 March and 24 April 1969, the period surrounding the inferior conjunction on 7 April. Extension of the observations over this interval was necessary in order that the tilt of the planet's apparent rotation axis would vary sufficiently to remove the degeneracy that occurred on a single day's observations for those regions separated by an integer number of interferometer fringes. This degeneracy is a consequence of the limited tracking imposed by the antennas, which did not permit sufficient change in the projected baseline to resolve this degeneracy in the course of a single day's observations. Since the echo intensity drops rapidly with increasing distance from the sub-Earth point, it proved useful to display the results as local departures from the mean scattering properties of the surface. From observations made in Arecibo in 1967 at 70 cm, Jurgens and Dyce (4) found that, for pulse lengths exceeding $500 \mu\text{sec}$, the average scattering properties were sufficiently well represented for the present purpose by Muhleman's scattering law (5), with $\alpha = 0.05$. Thus, each day's observations were normalized to the expected mean

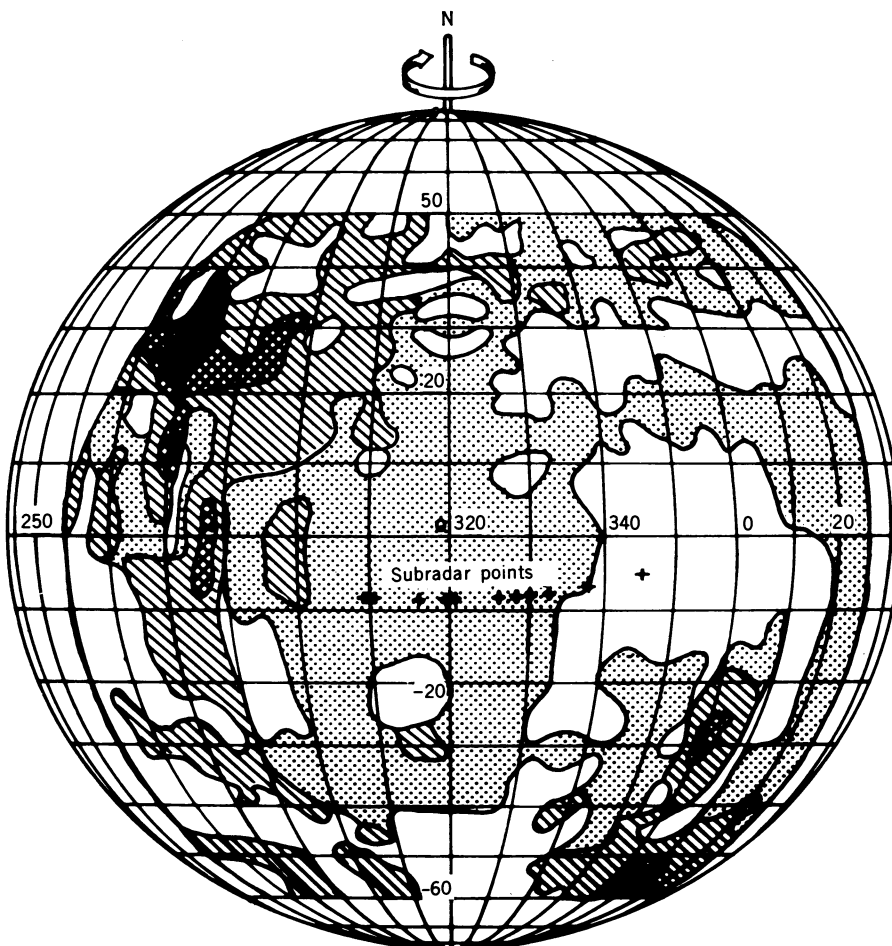


Fig. 2. Intensity contours derived from Fig. 1. Increasing scattering follows this order: dotted, hatched, cross-hatched, and darkened. The crosses give the positions of the subradar points for the 11 observations.

intensities at each value of delay and frequency as derived from Muhleman's law.

A new determination of the Venus rotation period and spin axis direction has recently been made by Jurgens (6) on the basis of feature positions measured between 1964 and 1969. These values, which we employed in this reduction, are 243.0 days for the rotation period, 272.7° for the right ascension of the northern axis, and +65.3° for its declination. The longitude reference was defined such that the 320° meridian contained the sub-Earth point at 0^h UT on 20 June 1964. Because our definitions of the rotation period and spin axis direction differ slightly from those of Rogers and Ingalls (2, 3), there is a difference of about 3° in the origin of longitude between the two systems (0° on their map corresponds approximately to 3° on ours).

The 11 maps were appropriately weighted and added together. The resultant composite map is shown as Fig. 1. Contours outline the major areas of differing contrast in Fig. 2. The areas above 40° latitude and below -50° latitude are tentative, as the signal-to-noise ratio was relatively poor in these regions. A number of regions whose reflectivity is significantly higher than that of their surroundings are apparent. Two of these, the region variously called α , F, or Faraday at -30° latitude, 0° longitude, and the β complex at 30° latitude, 280° longitude (seen under a different aspect angle this region separates into two features, which we have called Gauss and Hertz), have been observed with monostatic systems since 1964. Of major interest are the low-reflectivity features that are not normally apparent with monostatic systems because of the ambiguity problem.

These features seem to separate into two types: (i) large, irregularly shaped areas such as those centered on 27° latitude, 330° longitude to at least 30° longitude, and those centered on -20° latitude, 293° longitude; and (ii) circular features. The two circular features centered on 30° latitude, 320° longitude, and on -30° latitude, 337° longitude, seem to have a central feature reminiscent of some lunar craters, although they are approximately 1000 km in diameter. As was mentioned by Rogers and Ingalls (2), there is a temptation to equate the low-reflectivity features with lunar maria, which are smoother and have a lower reflectivity than the surrounding highlands. Such

an interpretation, however, will have to await observations in the depolarized receiving mode, where the predominant echo power arises from diffuse scattering.

Although agreement between the maps at the two wavelengths is good in respect to general boundaries between regions of differing reflectivity, the relative contrasts seem to differ markedly in some instances. For small features this difference may be partly due to the different resolutions used, since the 3.8-cm map had an area resolution approximately four times better than ours. The feature α or Faraday at -30° latitude, 0° longitude, which is resolved at both wavelengths, seems to have a considerably higher relative contrast at 3.8 cm than at 70 cm. This is the result either of greater roughness at a scale of 3.8 cm as compared with 70 cm or of increased elevation that would make atmospheric absorption at 3.8 cm considerably less than for the surrounding area of lower elevation.

Despite the considerable advance that the radar interferometer represents over other methods in mapping the surface scattering of Venus at radio wavelengths, we still know very little about the actual nature of the surface. Differences in the backscattered power may be due to changes in the small-scale roughness, mean slope, dielectric constant, or, in the case of wavelengths of less than 10 cm, in the surface height

(with the resultant change in atmospheric absorption). Observations in the depolarized mode would help greatly to resolve this problem, but, so far, little has been done in this direction because of the greater sensitivity required. Jurgens and Dyce (4) have reported observing a depolarized return from the β complex at 30° latitude, 280° longitude, and possibly from Faraday at -30° latitude, 0° longitude, which indicates that at least part of the enhancement of these regions is due to an increase in the roughness on the scale of 70 cm.

D. B. CAMPBELL

R. F. JURGENS, R. B. DYCE

F. S. HARRIS, G. H. PETTENGILL
Cornell-Sydney University Astronomy
Center, Arecibo Observatory,
Arecibo, Puerto Rico 00612

References and Notes

1. A. E. E. Rogers, T. Hagfors, R. A. Brockelman, R. P. Ingalls, J. L. Levine, G. H. Pettengill, R. S. Weinstein, *M.I.T. Lincoln Lab. Tech. Rep. 444* (1968).
2. A. E. E. Rogers and R. P. Ingalls, *Science* **165**, 797 (1969).
3. ———, *Radio Sci.* **5**, 425 (1970).
4. R. F. Jurgens and R. B. Dyce, *Astron. J.* **75**, 297 (1970).
5. D. O. Muhleman, *ibid.* **69**, 34 (1964).
6. R. F. Jurgens, *Radio Sci.* **5**, 435 (1970).
7. We thank I. Shapiro of the Massachusetts Institute of Technology and his staff for supplying the needed ephemerides, and the engineering staff of the Arecibo Observatory for their help in setting up the interferometer. The Arecibo Observatory is operated by Cornell University under contract to the National Science Foundation, with partial support from the Advanced Research Projects Agency.

14 September 1970

Lunar Surface: Changes in 31 Months and Micrometeoroid Flux

Abstract. *Comparison of pictures of the lunar surface taken 31 months apart by Surveyor 3 and Apollo 12 show only one change in the areas disturbed by Surveyor: a 2-millimeter particle, in a footpad imprint, that may have fallen in from the rim or been kicked in by an approaching astronaut. Vertical walls 6 centimeters high did not collapse and dark ejecta remained dark. No meteorite craters as large as 1.5 millimeters in diameter were seen on a smooth soil surface 20 centimeters in diameter; this indicates a micrometeoroid flux lower than 4×10^{-7} micrometeoroids per square meter-second at an energy equivalent to about 3×10^{-8} gram at 20 kilometers per second. This flux is near the lower limit of previous determinations.*

During the period from 20 April to 3 May 1967, the spacecraft Surveyor 3 sent to Earth thousands of television pictures of the lunar surface near its landing site in Oceanus Procellarum at 23.34°W longitude, 2.99°S latitude (ACIC coordinate system). On 20 November 1969, the site was visited by Apollo 12 astronauts Alan Bean and Charles Conrad, who took a number of pictures of the surface with a hand camera on 70-mm film. This provides

an opportunity to compare pictures of the same small areas of the lunar surface taken 31 months apart.

I have made a preliminary comparison, examining areas that had been disturbed by the Surveyor spacecraft. These disturbances produced markings in the lunar soil which were easily identifiable and simpler in shape than the irregularities, on a scale of centimeters and smaller, characteristic of the undisturbed lunar surface. Accordingly,